# Supporting Information

## Hart et al. 10.1073/pnas.1013168108

### SI Methods

**B-Cell Subsetting.** B-cell developmental stages in bone marrow were distinguished using the system of Hardy et al. (1) using the following criteria: fraction A [Lin−, B220+, CD43 (clone S7)+, CD24−, and BP-1−], fraction B (Lin−, B220+, CD43+, CD24+, and BP-1−), fraction C (Lin−, B220+, CD43+, CD24 Int, and BP-1+), fraction C′ (Lin−, B220+, CD43+, CD24 hi, and BP-1+), fraction D (Lin−, B220+, CD43−, and IgM−), fraction E (Lin−, B220 Int, CD43−, and IgM+), and fraction F (Lin−, B220 hi, CD43−, and IgM+) (1). Lineage (Lin) stains include CD4, CD8, and F4/80.

Peripheral B-cell subsets were defined with the following markers: bulk transitional (CD19+, B220+, and CD93+) and transitional subsets T1 (CD19+, B220+, CD93+, IgM hi, and CD23 lo), T2 (CD19+, B220+, CD93+, IgM hi, and CD23 hi), T3 (CD19+, B220+, CD93+, IgM lo, and CD23 hi) (2), marginal zone precursor (MZP; CD19+, B220+, CD93-, IgM hi, CD21 hi, and CD23 hi) (3), MZ (CD19+, B220+, CD93−, CD21 hi, and CD23 lo), follicular (CD19+, B220+, CD93−, CD21 Int, and CD23 hi), and B1 (CD19+, B220 Int/lo, CD43+, and IgM+), with B1a and B1b subsets being CD5-positive and -negative, respectively (4). Alternative stains for MZ cells include CD9 and CD1d as markers. For the assessment of λ+ B-cell populations, an antibody specific for Ig λ1-, λ2-, and λ3-light chains was used (Cat. no. 553434; BD Bioscience).

**Bone Marrow Calculations.** The CD45.1/CD45.2 vs. CD45.2 ratio of CD11b+ myeloid cell subsets was used to assess relative engraftment of the donor bone marrows. Mature bone marrow B cells were isolated from the femurs, which are estimated to contain 6.5% of total bone marrow (5); hence, the cell numbers for each subset were multiplied by 15.4 (100/6.5) to estimate total bone marrow numbers per mouse.

**Immunofluorescence.** Spleens were snap-frozen in OCT compound (Tissue-Tek) using a dry ice bath and were stored at −80 °C. The Leica DM5500B automated upright microscope has a high-precision motorized *x/y* stage and a Leica DFC340FX Digital Camera (Leica). Sections were stained with anti-IgM–FITC (Cat. no. 115–096-075; Jackson ImmunoResearch) and biotinylated anti-IgD (Clone: 11–26; eBioscience). Visualization of IgD was achieved using Cy3 Streptavidin (Cat. no. 43–4315; Invitrogen).

**Buffers/Media.** FACS Buffer is composed of PBS, 1% FCS, and 0.02% sodium azide (pH 7.2). Supplemented Roswell Park Memorial Institute (RPMI) 1640 is composed of 10% FCS, 5 mM Hepes, 50 U/mL Pen-Strep, 2 mM L-glutamate, 50 mM 2-mercaptoethanol, and 50 mg/mL gentamicin sulfate.

**Oligonucleotide Microarrays.** RNA (150–300 ng) was used for generating biotinylated cRNA through single-round amplification using the MessageAmpIII RNA Amplification kit (Ambion) following the manufacturer's recommendations. A total of 20 μg biotinylated cRNA was fragmented in 1× RNA fragmentation buffer (5× is 200 mM Tris acetate, pH 8.2, 500 mM potassium acetate, and 150 mM magnesium acetate) at 94 °C for 35 min followed by cooling on ice. The fragmented, biotinylated cRNA was hybridized to the Affymetrix murine 430 2.0 genechips (Affymetrix), washed, and scanned at the Biomedical Genomic Center (University of Minnesota) following standard procedures. Three independent RNA samples were analyzed.

**Microarray Analysis.** Microarray expression results were analyzed using GeneSpringGX 11.0 software (Agilent). A total of 45,101 probe sets were analyzed. Using the import of Affymetrix CEL files, a new experiment was created, and background correction, normalization, and probe summarization were performed using the MAS5 algorithm (for MAS5, genes with absent or no call in all samples were removed). Statistical analysis included an unpaired *t* test ($P \leq 0.05$), and an average fold-change (1.4-fold) cutoff was applied.


1. Hardy RR, Carmack CE, Shinton SA, Kemp JD, Hayakawa K (1991) Resolution and characterization of pro-B and pre-pro-B cell stages in normal mouse bone marrow. *J Exp Med* 173:1213–1225.
2. Allman D, et al. (2001) Resolution of three nonproliferative immature splenic B cell subsets reveals multiple selection points during peripheral B cell maturation. *J Immunol* 167:6834–6840.
3. Srivastava B, Quinn WJ 3rd, Hazard K, Erikson J, Allman D (2005) Characterization of marginal zone B cell precursors. *J Exp Med* 202:1225–1234.
4. Allman D, Pillai S (2008) Peripheral B cell subsets. *Curr Opin Immunol* 20:149–157.
5. Boggs DR (1984) The total marrow mass of the mouse: A simplified method of measurement. *Am J Hematol* 16:277–286.

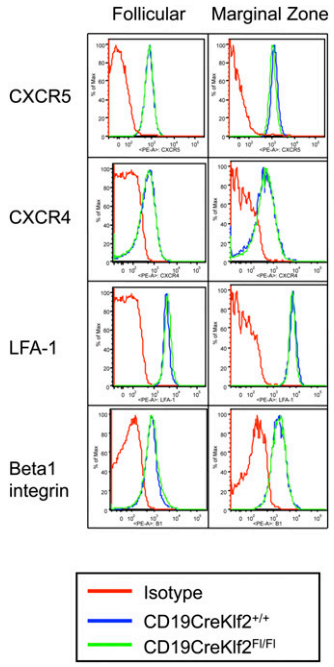


**Fig. S1.** Flow cytometric analysis for cell surface expression of CXCR5, CXCR4, LFA-1, and β1-integrin on follicular and marginal zone B cells from CD19CreKLF2$^{+/+}$ and CD19CreKLF2$^{Fl/Fl}$ mice.

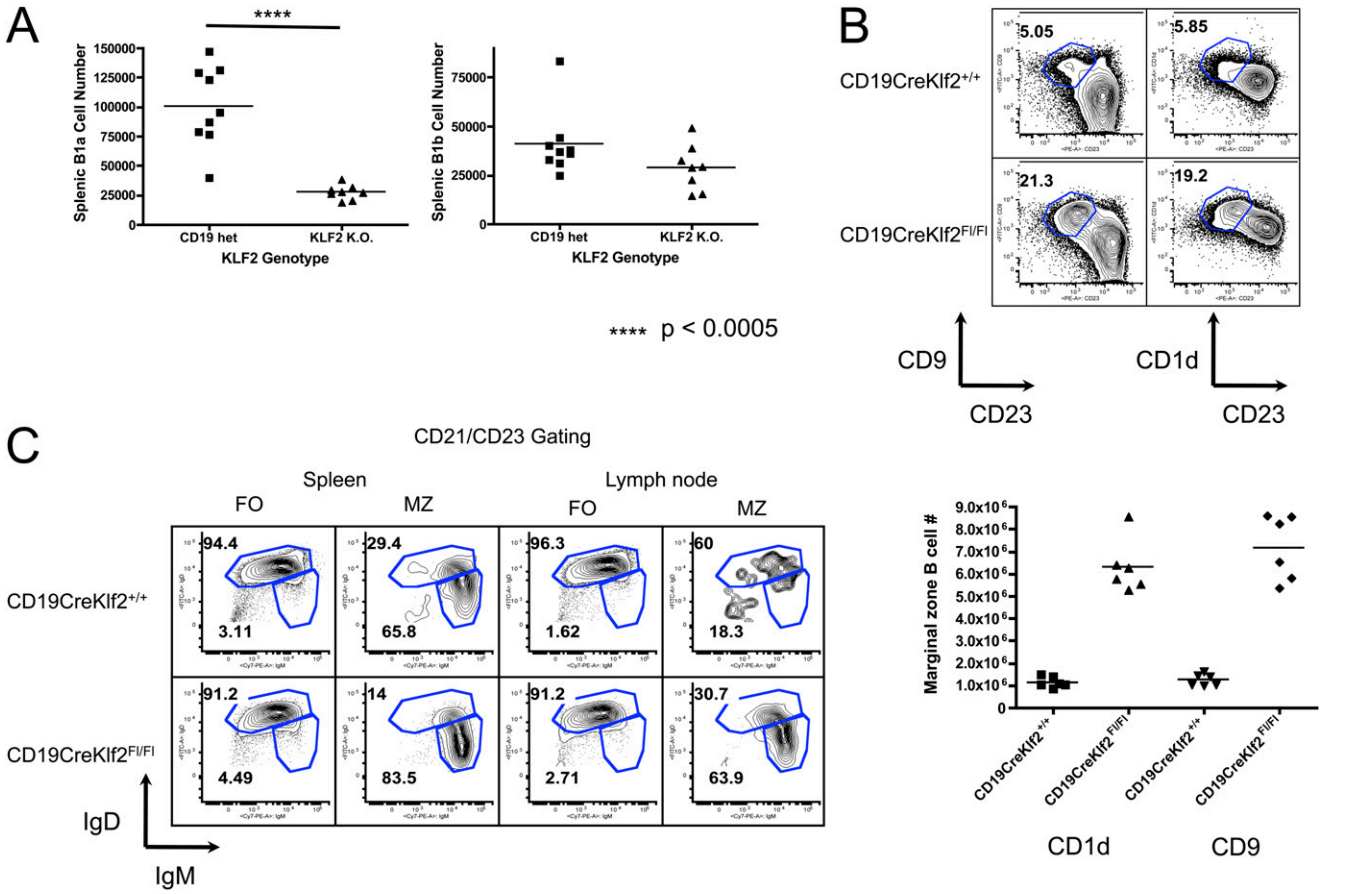


**Fig. S2.** (*A*) Numbers of splenic B1a (CD5+ CD19+, B220 Int/lo, CD43+, and IgM+) and B1b (CD5-, CD19+, B220 Int/lo, CD43+, and IgM+) cells in control (CD19het) and KLF2-deficient (KLF2 KO) mice. (*B*) CD19+, B220+, and CD93- cells were examined for expression of CD9 or CD1d vs. CD23. Typical marginal zone (MZ) B cells are CD9+, CD1d+, and CD23- (MZ) cells. *Upper* shows the frequency of mature splenic B cells, whereas *Lower* shows numbers of MZ phenotype cells defined with CD1d or CD9, as indicated. (*C*) Follicular (FO) or MZ phenotypes in spleen and lymph nodes were first gated using CD19+, B220+, CD93-, CD21, and CD23 (Fig. 3). The cells falling in the FO and MZ gated cells were then assessed for expression levels of IgM and IgD.

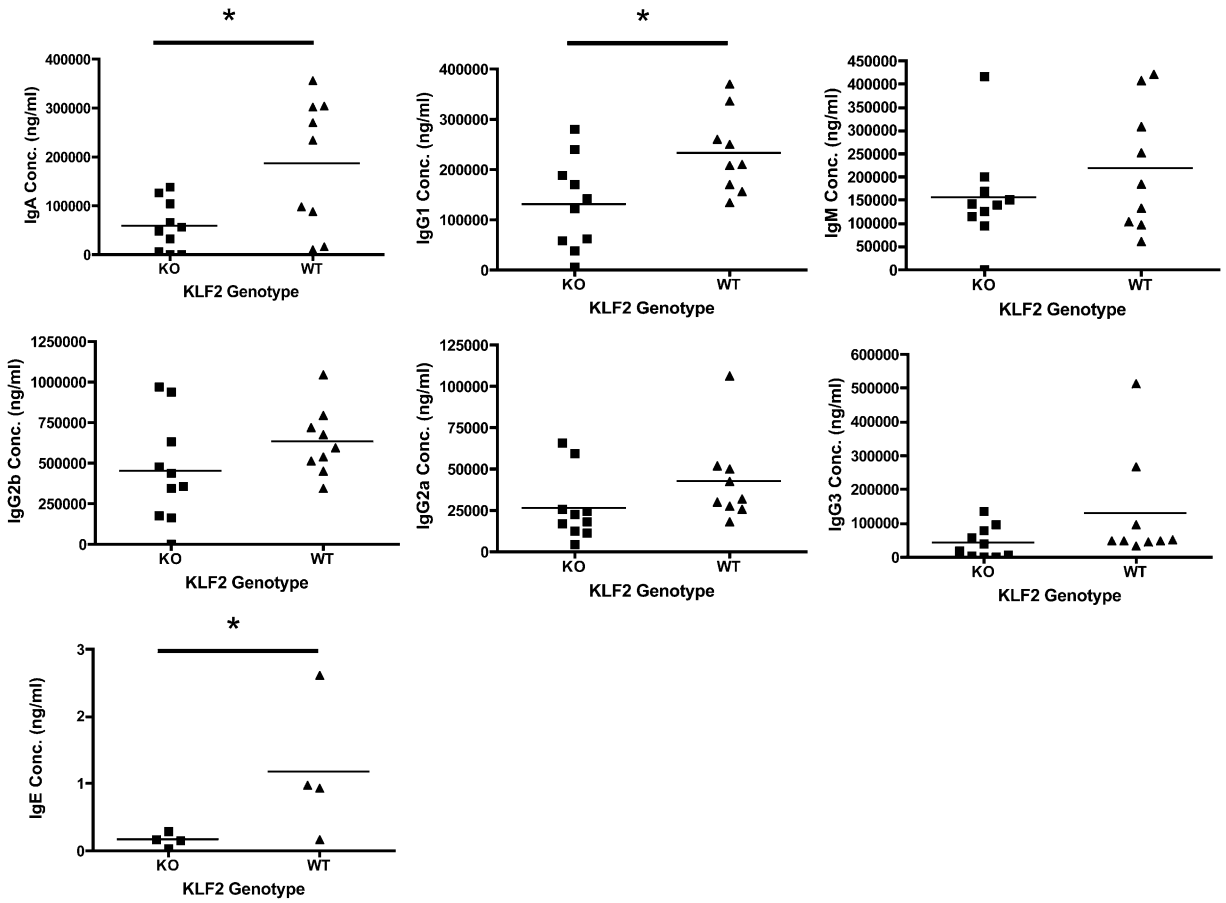


**Fig. S3.** Serum from unimmunized CD19CreKLF2$^{+/+}$ and CD19CreKLF2$^{Fl/Fl}$ mice was assessed for the indicated antibody isotypes levels. Mice were 2–8 mo of age for this analysis. Asterisk indicates a $P$ value $< 0.05$

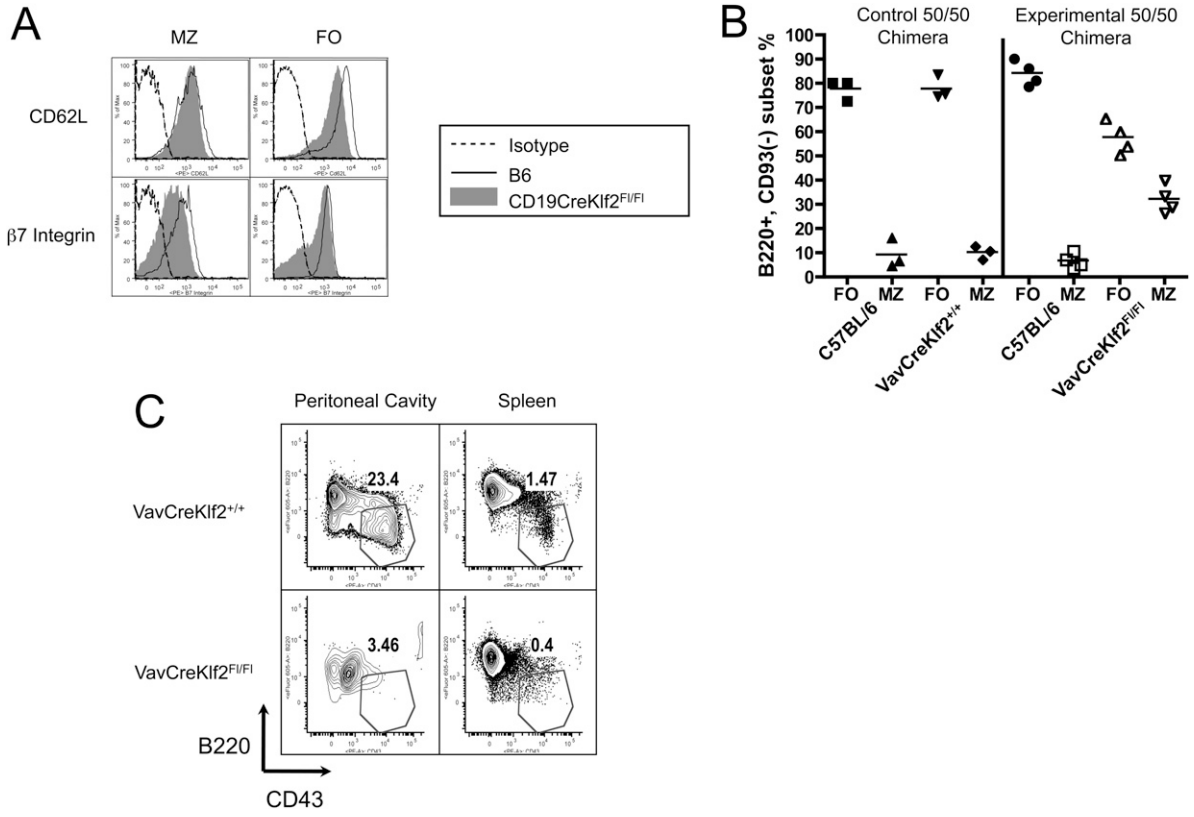


**Fig. S4.** (*A*) FO and MZ frequencies from mixed chimeras showed a significant MZ cell increase for only Vav-Cre KLF2 KO cells, where Vav-Cre is an earlier expressed transgenic B cell conditional cre relative to CD19 Cre. Cre control mixed chimeras had one-half C57BL/6 (B6) CD45.1/2 double +ive and one-half VavCreKLF2$^{+/+}$ (experimental) CD45.2 +ive donor bone marrow into a B6 CD45.1+ive host ($n$ = 3). KLF2 KO mixed chimeras had the same setup except that the experimental one-half also had KLF2$^{FI/FI}$ ($n$ = 4). This setup allows all donor and host hematopoietic populations to be identified. (*B*) CD62L and b7-integrin expression from each population in a mixed B6/CD19Cre*Klf2*$^{fl/fl}$ chimeric mouse. Each population was identified by its congenic CD45.1/2 or CD45.2 marker, respectively, and subsequent subset (Fig. 3). (*C*) The frequency of B1 phenotype cells was determined (Fig. 2) in VavCreKLF2$^{+/+}$ and VavCreKLF2$^{fl/fl}$ mice. Representative of two experiments and four mice.

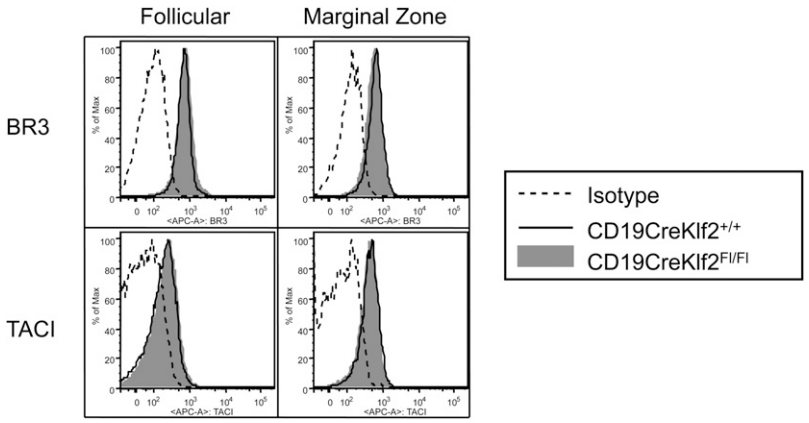


**Fig. S5.** Expression levels for the BAFF receptors BR3 and TACI were determined in control and CD19CreKlf2$^{fl/fl}$ mice. Representative of three experiments.

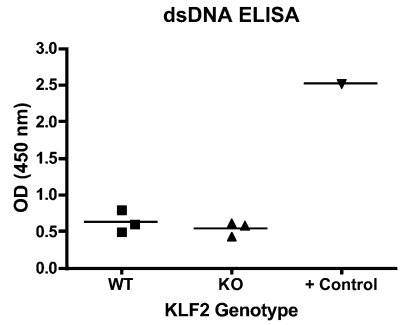


**Fig. S6.** Serum from 12-mo-old CD19CreKlf2$^{+/+}$ and CD19CreKlf2$^{Fl/Fl}$ was tested for the presence of anti-dsDNA antibodies along with serum from a 6-mo MRL-LPR mouse as a positive control. No significant level of dsDNA antibodies or difference between CD19CreKlf2$^{+/+}$ and CD19CreKlf2$^{Fl/Fl}$ was found.

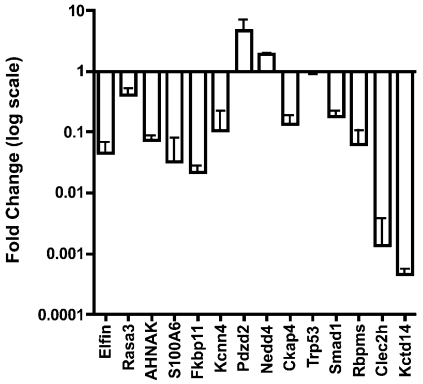


**Fig. S7.** Gene expression analysis was performed on sorted KLF2-deficient and control FO B cells using real-time RT-PCR similar to Fig. 2*E* for the indicated genes. The fold change between CD19CreKlf2$^{Fl/Fl}$ and CD19CreKlf2$^{+/+}$ FO B cells is indicated.

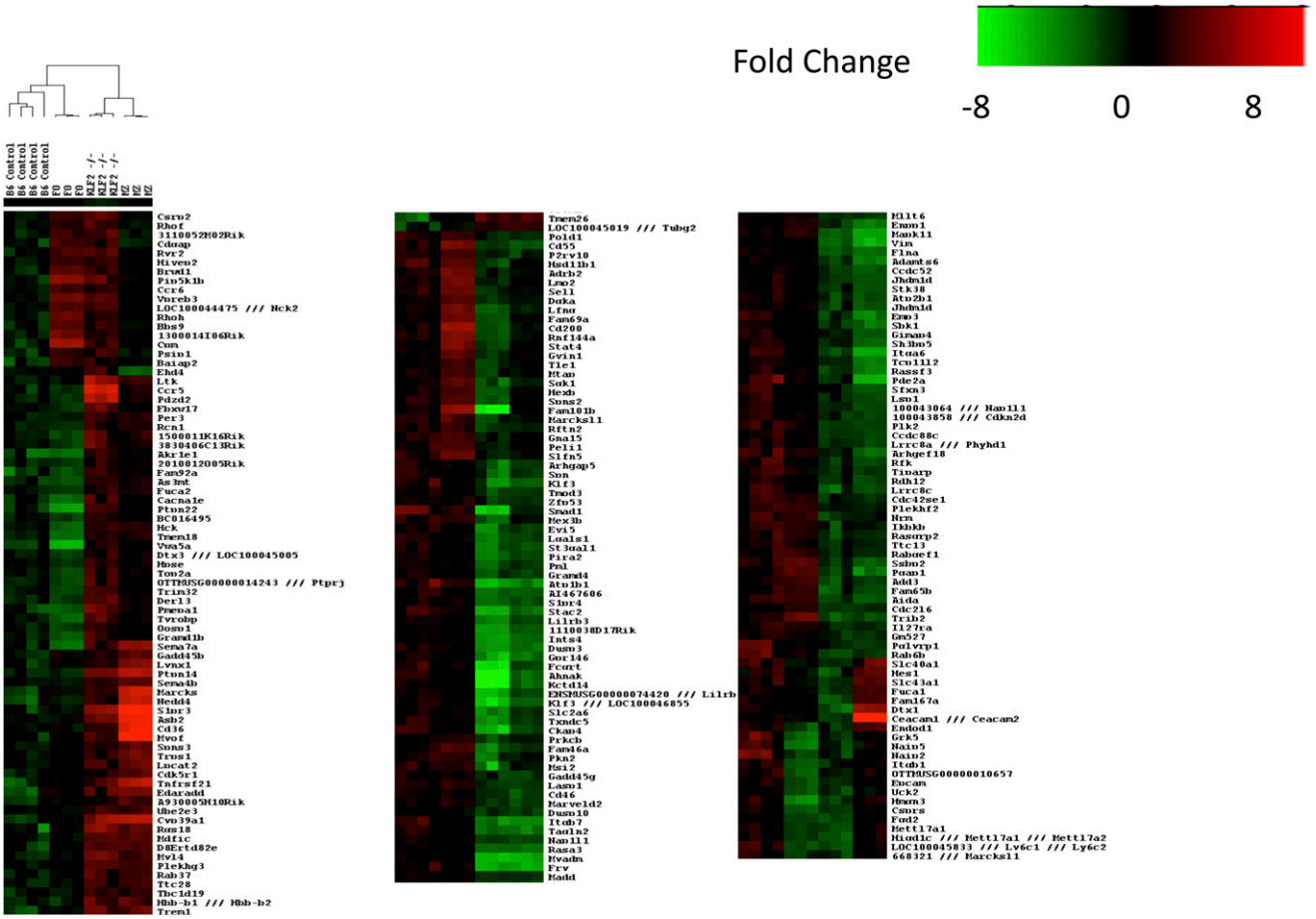


**Fig. S8.** Cluster analysis of different WT and B-cell populations. Genes that were identified as differentially expressed between CD19CreKlf2$^{Fl/Fl}$ and CD19CreKlf2$^{+/+}$ FO B cells (using a significance cut-off of $P < 0.05$ and a fold change of >1.4) were selected after analysis in GeneSpring software. The same analysis and criteria were used to identify differentially expressed genes between normal FO and MZ cells from the public Gene Expression Omnibus database (http://www.ncbi.nlm.nih.gov/geo/). The genes that were differentially expressed in both pair---wise comparisons were used to drive the cluster analysis. Note that the KLF2-deficient FO B cells cluster between normal FO and MZ B cells, sharing characteristics of both pools. Some changes are observed between normal and CD19CreKlf2$^{+/+}$ FO B cells, presumably reflecting effects of CD19 heterozygosity.